Available online at www.sciencedirect.com
ScienceDirect
Journal of Magnetism and Magnetic Materials 320 (2008) e446–e449
Journal of magnetism and magnetic materials
www.elsevier.com/locate/jmmm

Local magnetic moments and hyperfine fields of transition element impurities in ferromagnetic Gd and Tb rare earth metals

A.L. de Oliveira[a], M.V. Tovar Costa[b,*], N.A. de Oliveira[c], A. Troper[c,d]

[a]Centro Federal de Educação Tecnológica de Química de Nilópolis, Rua Lúcio Tavares, 1045, Nilópolis-RJ, 26530-060, Brazil
[b]Instituto de Aplicaçao, Universidade do Estado do Rio de Janeiro, Rua Santa Alexandrina, 288, Rio de Janeiro, 20261-232, Brazil
[c]Instituto de Física, Universidade do Estado do Rio de Janeiro, Rua São Francisco Xavier, 524, Rio de Janeiro, 20550-013, Brazil
[d]Centro Brasileiro de Pesquisas Físicas, Rua Dr. Xavier Sigaud, 150, Rio de Janeiro, 22290-180, Brazil

Available online 18 March 2008

Abstract

We discuss the formation of the local magnetic moments and the related magnetic hyperfine fields at *n*d ($n = 3, 4, 5$) transition impurities diluted in ferromagnetic Gd and Tb metals. The *n*d impurities are described within the Wolff–Clogston picture and the mean field approximation is adopted to deal with the Coulomb-like interaction. The next-neighbor tunneling, due to the translational invariance breaking introduced by the impurity, is also included in this work. Following a self-consistent procedure and using a criterious physical choice of parameters, we are able to calculate the local magnetization and magnetic hyperfine fields at the impurity sites. The calculated hyperfine fields are in good agreement with the experiments.

PACS: 75.30.Hx; 71.20.Eh

Keywords: Gd and Tb metals; Magnetic hyperfine field; Local magnetic moment

One important problem in condensed matter physics is the study of the magnetic moment formation in metals and their relations to hyperfine fields [1–5]. Here we address a theoretical study of the substitutional nd impurities diluted in ferromagnetic rare earth Gd and Tb metals.

We begin by describing the rare earth Gd and Tb hosts. It is well established that in the rare earth metals the 5d and 6s electrons form delocalized s–d bands whereas the 4f electrons are localized. The main contribution to the magnetic moment as well as to the hyperfine field comes from the localized states. However, the s–p and d electrons play an important role in carrying on the information along the material, via a Rudermann–Kittel–Kasuya–Yosida (RKKY) mechanism. The saturation magnetic moment of Gd is $7.63\,\mu_B$ where $7.0\,\mu_B$ is ascribed to the 4f electrons and $0.63\,\mu_B$ to the conduction ones. It is also observed that for Tb metals at low temperatures a saturation magnetic moment of $9.34\,\mu_B$ appears with $0.34\,\mu_B$ due to the 5d conduction electrons [6].

The rare earth features mentioned above are well described by the following model Hamiltonian:

$$H_0 = \sum_{j,\sigma}[\varepsilon_c^H - \sigma h_c^f]c_{j\sigma}^\dagger c_{j\sigma} + \sum_{j,l,\sigma} t_{lj}^{cc} c_{j\sigma}^\dagger c_{l\sigma} + \sum_{j,l,\sigma} t_{lj}^{dd} d_{j\sigma}^\dagger d_{l\sigma} + \sum_{j,\sigma}[\varepsilon_d^H - \sigma h_d^f]d_{j\sigma}^\dagger d_{j\sigma} + U_d^H \sum_j n_{j\uparrow}^d n_{j\downarrow}^d, \quad (1)$$

where $\varepsilon_c^H(\varepsilon_d^H)$ is the energy of the center of the s–p (d) host band. U_d^H is the host Coulomb interaction parameter. The terms $h_c^f = \frac{1}{2}J_{cf}J_{0z}^f$ and $h_d^f = \frac{1}{2}J_{df}J_{0z}^f$ are the local host magnetic field acting at each host site yielding a band splitting. $J_{cf}(J_{df})$ is the exchange interaction parameter and J_{0z}^f is the total rare earth angular moment.

Due to a host translational symmetry broken induced by the addition of a substitutional impurity, a set of changes in Eq. (1) is necessary. First, in the Coulomb interaction, i.e., $U_d^I \neq U_d^H$; second, the hopping t_{0l} is quite different from that of host sites t_{jl} and also, a change in the local energy band centers appears ($\varepsilon_c^I \neq \varepsilon_c^H$, $\varepsilon_d^I \neq \varepsilon_d^H$).

*Corresponding author. Tel.: +55 21 2141 7285; fax: +55 21 2141 7400.
E-mail address: mvtcosta@gmail.br (M.V. Tovar Costa).

0304-8853/$ - see front matter © 2008 Published by Elsevier B.V.
doi:10.1016/j.jmmm.2008.02.189

Treating the Coulomb interaction via the Hartree–Fock approximation, the total Hamiltonian reads as

$$H = H_0^c + H_0^d + V_\sigma^c + V_\sigma^d, \tag{2}$$

with $H_0^c + H_0^d$ corresponding to the pure host defined in Eq. (1). V_σ^c and V_σ^d represent the s–p and d potentials, respectively, and are given by

$$V_\sigma^\beta = V_{0\sigma}^\beta + \tau_\beta \sum_{j\neq 0,\sigma} (\beta_{0\sigma}^\dagger \beta_{j\sigma} + \beta_{j\sigma}^\dagger \beta_{0\sigma}), \tag{3}$$

where $\beta = c$ or d with

$$V_{0\sigma}^c = [\Delta\varepsilon_c - \sigma\lambda_c\varepsilon_c] c_{0\sigma}^\dagger c_{0\sigma} \tag{4}$$

and

$$V_{0\sigma}^d = [\Delta\varepsilon_d + \Delta U\langle n_{-\sigma}^d\rangle + U^1\delta\langle n_{0-\sigma}^d\rangle - \sigma(\bar{h}_d^f - h_d^f)] \times d_{0\sigma}^\dagger d_{0\sigma}. \tag{5}$$

$\Delta\varepsilon_c = \varepsilon_c^{\mathrm{I}} - \varepsilon_c^{\mathrm{H}}$, $\Delta\varepsilon_d = \varepsilon_d^{\mathrm{I}} - \varepsilon_d^{\mathrm{H}}$, τ_c (τ_d) is a proportionality factor estimated from impurity and host atomic wave functions [7–9] and λ_c is the ratio between impurity and host band splitting. In this approximation, we consider only intraband s−p ⇌ s−p and $d \rightleftharpoons d$ effective scattering potentials V_σ^c and V_σ^d. These potentials are obtained in such a way that the s–p impurity electrons are screened by the s–p host conduction band, whereas the impurity d-electrons are screened by the d-conduction band. So, one has two-independent Koster–Slater problems, namely: (i) An extended Daniel–Friedel impurity problem [10–12], which leads to the calculation of the s–p local magnetization, (ii) an extended Campbell–Gomes problem [5], which leads to the calculation of the d local magnetic moment. Using Dyson's equation, the impurity on-site Green's function associated to the Hamiltonian (2) is

$$G_{00\sigma}^{\beta\beta}(z) = \frac{g_{00\sigma}^{\beta\beta}(z)}{\alpha_\beta^2 - g_{00\sigma}^{\beta\beta}(z)[(\alpha_\beta^2 - 1)(z - \varepsilon_{\mathrm{h}\beta}) + V_{0\sigma}^\beta]}, \tag{6}$$

where $z = \varepsilon + \mathrm{i}0$, $\alpha_\beta = \tau_\beta + 1$ and $g_{00}^\beta(z)$ is the pure β-band of the host. The change in the occupation, ΔZ_σ^β, of s–p and d spin states, respectively are obtained by integrating the change in the density of states at the origin

$$\Delta\rho_\sigma^\beta = -\frac{1}{\pi}\mathrm{Im}(G_{00\sigma}^{\beta\beta}(z) - g_{00\sigma}^{\beta\beta}(z)), \tag{7}$$

up to the Fermi level ε_{F}. The result reads

$$\Delta Z_\sigma^\beta = -\frac{1}{\pi}\mathrm{Im}\ \ln\{\alpha_\beta^2 - g_{00\sigma}^{\beta\beta}(\varepsilon_{\mathrm{F}}) \times[(\alpha_\beta^2 - 1)(\varepsilon_{\mathrm{F}} - \varepsilon_{\mathrm{h}\beta}) + V_{0\sigma}^\beta]\}. \tag{8}$$

To impose the total charge neutrality condition, $V_{0\sigma}^\beta$ is self-consistently determined using the extended Friedel's sum rule $\Delta Z^\beta = \Delta Z_\uparrow^\beta + \Delta Z_\downarrow^\beta$ [7–9]. Then, we are able to get the magnetic moment at the impurity site making use of the following equation:

$$\tilde{m}_\beta(0) = p\sum_\sigma \sigma\tilde{n}_{0\sigma}^\beta = -p\sum_\sigma \frac{\sigma}{\pi}\int_{-\infty}^{\varepsilon_{\mathrm{F}}} \mathrm{Im}\{G_{00\sigma}^{\beta\beta}(z)\}\,\mathrm{d}z, \tag{9}$$

where the factor $p = 4$ or 5 accounts for the degeneracy of the s–p and d states, respectively. The total hyperfine magnetic field $B_{\mathrm{hf}}^{\mathrm{total}}$ is given by

$$B_{\mathrm{hf}}^{\mathrm{total}} = A(Z_{\mathrm{imp}})\tilde{m}_c(0) + A_{\mathrm{cp}}^d\tilde{m}_d(0), \tag{10}$$

where $A(Z_{\mathrm{imp}})$ is the Fermi–Segrè coupling and A_{cp}^d is a core polarization coupling parameter, which is constant for a given *n*d series, both estimated by Campbell [10].

In what follows we present the results of self-consistently calculated magnetic moment and the magnetic hyperfine fields for *n*d impurities in Gd (Figs. 1 and 2) and Tb (Figs. 3 and 4) hosts. The s–p (conduction electron polarization) and d (core electron polarization) contributions are individually presented.

As seen from Eq. (10), the total magnetic hyperfine fields exhibit a competition between contributions $A_{cp}^d\tilde{m}_d(0)$ and $A(Z)\tilde{m}_c(0)$. Since Gd and Tb can be considered as ferromagnetic transition metals in the beginning of the 5d series (at very low temperatures), the calculations of the d-magnetic moments are always negative (with the possible exception of Lu Gd). On the other hand, the systematics of the d-magnetic moments in *n*d impurities diluted in the 3d ferromagnetic metals Fe [8] and Co [9] exhibit a change of sign behavior around the middle of the series. This is because in the case of ferromagnetic 3d hosts one has a repulsive charge potential acting on the host d-band given rise to an extracted bound state lying above the Fermi level; then changing the impurity local d-magnetic moment. In the case of 5d ferromagnetic Gd and Tb metals, one has the appearance of an attractive charge potential, which can give rise to a d-bound state lying below the extended d-band, thus maintaining the same sign of the d-magnetic moment along the series.

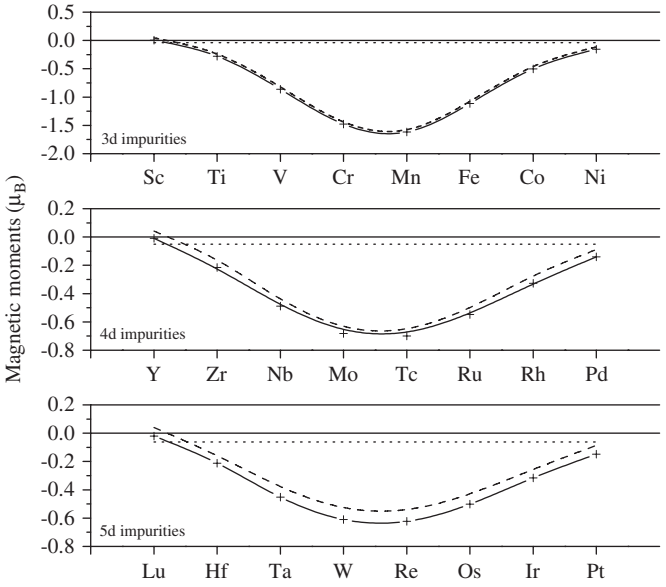

Fig. 1. Calculated local magnetic moments for the *n*d series impurities in Gd. Solid lines correspond to the total local magnetic moment, whereas dotted and dashed curves correspond to s–p and d contributions, respectively.

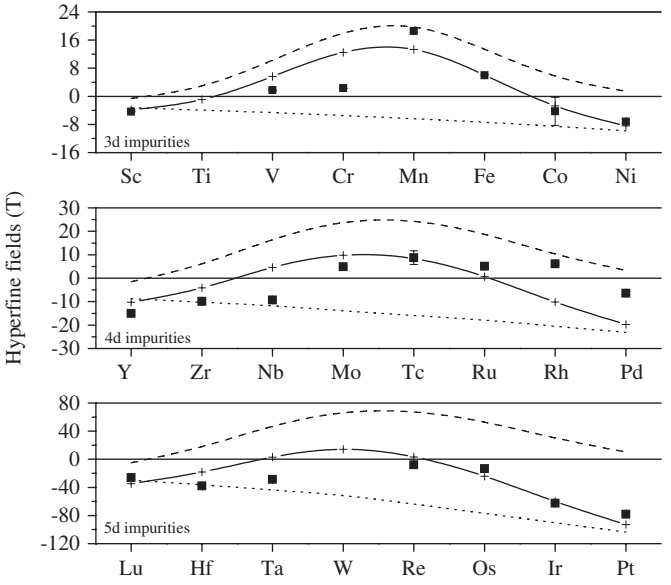

Fig. 2. Calculated hyperfine fields for the *n*d series impurities in Gd. Dotted and dashed lines correspond to s–p and d contributions to the total hyperfine fields, respectively. Solid line shows the total hyperfine fields [19] whereas square symbols are the experimental data [13].

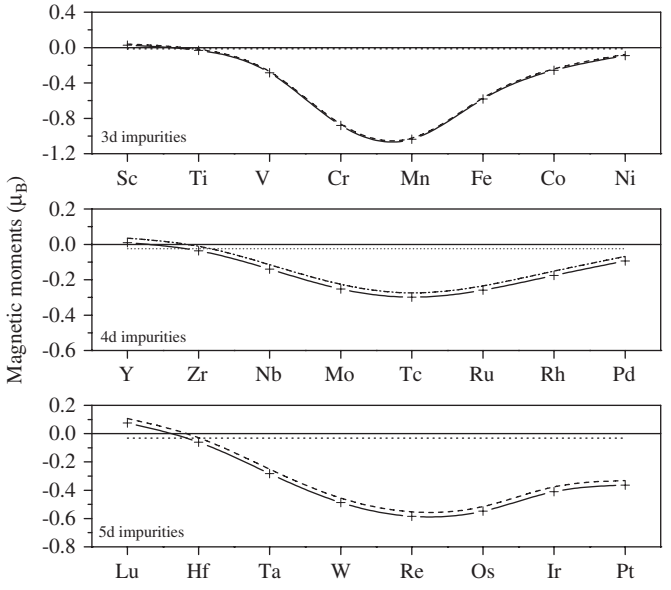

Fig. 3. Calculated local magnetic moments for the *n*d series impurities in Tb. Solid lines correspond to the total local magnetic moment, whereas dotted and dashed curves correspond to s–p and d contributions, respectively.

As far as the s–p magnetic moments are concerned, the calculations show that they are very small, not contributing substantially to the total magnetic moment. This is not true for the total magnetic hyperfine field since the presence of the term $A(Z)\tilde{m}_c(0)$ implies a change of the sign behavior of the total magnetic hyperfine field.

From Figs. 2 and 4 one observes that, the conduction electron polarization contribution $A(Z_{\mathrm{imp}})\tilde{m}_c(0)$ is always negative, whereas the core electron contribution $A^d_{\mathrm{cp}}\tilde{m}_d(0)$

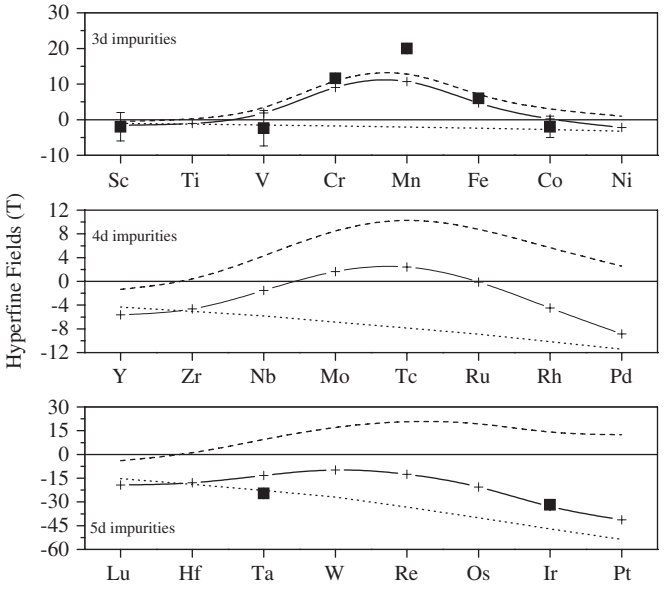

Fig. 4. Calculated hyperfine fields for the *n*d series impurities in Tb. Dotted and dashed lines correspond to s–p and d contributions to the total hyperfine fields, respectively. Solid line shows the total hyperfine fields [19] whereas square symbols are the experimental data [14–18]. Since we do not have experimental data for the 4d impurities, we exhibit only our theoretical self-consistent calculation.

has a change of sign behavior. The total magnetic hyperfine field for 3d impurities exhibit always a change of sign behavior in Gd and Tb. On the other hand, in the case of 5d impurities the total hyperfine field is always negative. This is quite clear in the Tb case, whereas in the Gd case all the experimental data as well as our calculations furnishes small negative values, approaching zero in the middle of the series. In particular, one predicts that the total hyperfine field in W Gd has a near zero value.

The calculated hyperfine fields exhibit a remarkable feature as a function of the impurity metal, as it is displayed in Figs. 2 and 4. The results follow the same trend of experimental data (square symbols). One may notice the double change of sign along the *n*d series for both studied materials. As *n* goes from 3 to 5 the sign change was found to disappears gradually. The calculated hyperfine fields for *n*d series presented above are in a fairly agreement with available experimental data [13–18], showing the good tendency of our results.

We would like to thank Conselho Nacional de Desenvolvimento Científico e Tecnológico - CNPq for financial support.

References

[1] J. Friedel, Nuovo Cimento Suppl. 7 (1958) 287.
[2] A. Wolff, Phys. Rev. 124 (1961) 1030.
[3] A.M. Clogston, B.T. Matthias, N. Peter, H.J. Williams, E. Orenzwit, R.J. Sherwood, Phys. Rev. 125 (1962) 541.
[4] J. Kanamori, J. Appl. Phys. 16 (1965) 929.
[5] I.A. Campbell, A.A. Gomes, Proc. Phys. Soc. (London) 91 (1967) 319.

[6] B. Coqblin, Electronic Structure of Rare Earth Metals and Alloys: The Magnetic Rare Earth, Academic Press, New York, 1977.
[7] J.F. van Acker, W. Speier, J.C. Fuggle, R. Zeller, Phys. Rev. B 43 (1991) 13916.
[8] N.A. de Oliveira, A.A. Gomes, A. Troper, Phys. Rev. B 52 (1995) 9137.
[9] W.N. de Freitas, A.L. de Oliveira, N.A. de Oliveira, A. Troper, J. Magn. Magn. Mater. B 226 (2001) 391.
[10] I.A. Campbell, J. Phys. C 2 (1969) 1338.
[11] C.E. Leal, A. Troper, J. Appl. Phys. 67 (1990) 5876.
[12] A.L. de Oliveira, M.V. Tovar Costa, N.A. de Oliveira, A. Troper, J. Appl. Phys. 81 (1997) 4215.
[13] G.N. Rao, Hyperfine Interactions 24–25 (1985) 1119.
[14] M. Forker, K. Krien, F. Reuschenbach, Hyperfine Interactions 9 (1981) 255.
[15] M. Forker, K. Krusch, Hyperfine Interactions 9 (1981) 399.
[16] M. Forker, R. Trzcinski, T. Merzhäuser, Hyperfine Interactions 15–16 (1983) 273.
[17] J. Boysen, J. Grimm, A. Kettschau, W.D. Brewer, G.V. Wilson, Phys. Rev. B 35 (1987) 1500.
[18] W.D. Brewer, S. Hauff, D. Jones, S. Frota-Pessoa, J. Kapoor, Y. Li, A. Metz, D. Riegel, Phys. Rev. B 51 (1995) 12595.
[19] A.L. de Oliveira, M.V. Tovar Costa, N.A. de Oliveira, A. Troper, J. Magn. Magn. Mater. 272–276 (2004) 639.